Intense Terahertz Excitation of Semiconductors

S.D. Ganichev
Terahertz Center, University of Regensburg, 93040, Regensburg, Germany

Abstract: The potential of the terahertz spectroscopy at high excitation level is demonstrated on the example of the recently observed new class of spin dependent elects: spin photocurrents. Two electsresponsible for the occurrence of an electric current caused by homogeneous excitation with terahertz radiation and linked to a uniform spin polarization in a QW are reviewed: the circular photogalvanic elect and the spin-galvanic elect. PACS numbers: 73.21.Fg, 72.25.Fe, 78.67.De, 73.63.Hs

Keywords: Terahertz，THz spectroscopy

doi: 10.11906/TST.136-160.2008.09.13

1. Introduction

With the development and application of molecular optically pumped terahertz lasers and free electron lasers the terahertz spectroscopy at high-excitation level be-came reality and received a great deal of attention recently [1]. High power terahertz (THz) lasers, tunable in the frequency range from 120 GHz to 30 THz, provide nanosecond pulses of electromagnetic radiation with intensity up to several MW/cm^2 corresponding in vacuum to electric field strengths of tens of kilovolts per centimeter. These THz electric fields are sufficient to lift semiconductors into an extremely nonlinear regime, well beyond the perturbative limit. Application of the high power THz radiation, gives rise to a variety of nonlinear phenomena in semiconductors, such as, tunneling, multiphoton absorption, light impact ionization, absorption saturation, etc. The characteristics of these effects differ substantially from their counterparts observed both in the visible and infrared ranges and in the range extending from microwaves to dc electric fields. This is due to the fact that in THz range the interaction in the electron-photon system undergoes a transition from the quantum to classical limit. Furthermore, high radiation intensity allows one to explore nonlinear dynamics or that sacrifice incident power to recover the linear response of systems with a small cross-section.

The potential of the THz spectroscopy at high excitation level is demonstrated on the example of the recently observed new class of spin dependent elects: spin-photocurrents. Terahertz experiments demonstrated that a homogeneous nonequilibrium spin polarization of electron gas drives an electric current in semiconductor quantum well (QW) structures. In this paper we introduce two photocurrents observed in QWs based on various semiconductor materials: the spin-galvanic effect (SGE), the circular photogalvanic effect (CPGE) and the magneto-gyrotropic elect (for reviews see [1–3]).

The spin of electrons and holes in solid state systems is an intensively studied quantum mechanical property as it is the crucial ingredient for semiconductor based spintronics and spin-optoelectronics (for recent reviews see [4–8]). The transport of the spin of charge carriers in semiconductor QWs is one of the key problems in this field. The necessary conditions to realize spintronic devices are high spin polarization in QWs, long spin relaxation times and a

large spin-splitting of subbands in k-space. The latter is important for the ability to control spins with an external electric field by the Rashba effect [9]. One of the most frequently used and powerful methods of generation and investigation of spin polarization is optical orientation [10]. Besides purely optical phenomena like circularly-polarized photoluminescence, the optical generation of an unbalanced spin distribution in a semiconductor may lead to spin photocurrents.

Circularly polarized light propagating through a gyrotropic [11] semiconductor or semiconductor quantum well (QW) structure and acting upon mobile carriers can generate a helicity-dependent dc electric current, undershort-circuit condition, or a voltage, in the case of open-circuit samples [2]. Appearance of these currents demonstrates a new property of the electron spin in a homogeneous and spin-polarized two-dimensional electron gas: its ability to drive an electric current if some general symmetry requirements are met. On a microscopical level the current flow is driven by an asymmetric distribution of spin polarized carriers in k-space of systems with lifted spin degeneracy due to k-linear terms in the Hamiltonian. The absorption of circularly polarized light results in optical spin orientation due to the transfer of the angular momentum of photons to electrons of a two-dimensional electron gas (2DEG). In quantum wells belonging to one of the gyrotropic crystal classes a non-equilibrium spin polarization of uniformly distributed electrons cause adirected motion of electron in the plane of the QW. These effects can be described by simple analytical expressions derived from a phenomenological theory. The requirement of gyrotropy rules out effects depending on the helicity of the radiation field in bulk optically non-active materials like bulk zinc-blende and diamond structure crystals. The reduction of dimensionality as realized in QWs makes spin photocurrents possible. A characteristic feature of this electric current, which occurs in unbiased samples, is that it reverses its direction upon changing the radiation helicity from left-handed to right handed and vice versa. The circular photogalvanic effect is caused by the asymmetry of the momentum distribution of carriers excited in optical transitions which are sensitive to the light circular polarization due to selection rules [12]. The spin-galvanic effect is a result of spin relaxation and in general does not need optical excitation; however it may also occur due to optical spin orientation[13,14].Most recently observed inverse spin galvanic effect predicted in [16–18] demonstrates that in gyrotropic non-magnetic QWs electric current always results in a spin orientation [19–21] .

In an external magnetic field spin photocurrents in gyrotropic low dimensional structures may be generated even by unpolarized radiation as it has been proposed for bulk gyrotropic crystals [22, 23]. The magneto-gyrotropic effect appear in the presence of an external n-plane magnetic field and is caused by k-linear terms in electron-phonon interaction resulting in asymmetric excitation or asymmetric energy relaxation of heated by THz radiation spin polarized electron gas [15, 24-26].This results show that, without a magnetic field, non-equilibrium free carrier heating can be accompanied by spin flow i.e. in a pure spin currents.

Spin photocurrents provided an experimental access for investigation of spin dependent properties of QWs, in particular to spin-splitting of subbands in *k*-space which allow to manipulate spins with an external electric field by the Rashba effect (for reviews see [2, 27,

28]). SGE and CPGE give an easy and direct method for investigation of the Rashba/Dresselhaus spin splitting of sub-bands [29, 30]. Furthermore, spin photocurrents allow investigation of spin relaxation processes [31, 32], provide methods to conclude on the symmetry of QWs [2, 33] and has also been utilized to develop fast THz detectors of radiation helicity [34].

While spin photocurrents may occur at visible excitation there is a particular interest in spin photocurrents generated by THz radiation. This is mostly caused by two reasons. First of all, in the THz range spin photocurrents may be observed and investigated much easier than in the visible range where strong spurious photocurrents due to other mechanisms like the Dember effect, photo-voltaic effects at contacts etc. mask the relatively weak spin photocurrents. Secondly, in contrast to conventional methods of optical spin orientation using inter-band transitions [10], THz radiation excites only one type of charge carriers yielding monopolar spin orientation [2, 35-37]. A substantial portion of investigations of the spin lifetime in semiconductor devices are based on optical spin orientation by inter-band excitation and further tracing the kinetics of polarized photoluminescence [5, 6, 8]. These studies give important insights into the mechanisms of spin relaxation of photoexcited free carriers. In contrast to these methods of optical spin orientation, monopolar spin orientation allows to study spin relaxation with-out electron-hole interaction and exciton formation in the conditions close to the case of electric spin injection.

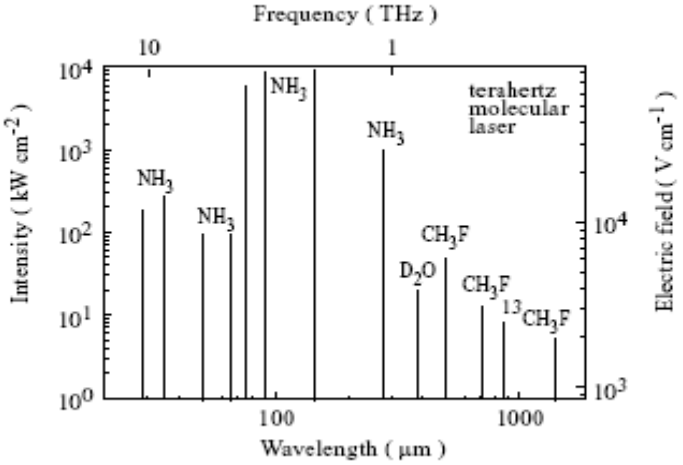

Fig. 1 Wavelength distribution of a set of strong laser lines in the terahertz (after [1]).

2. Experimental Technique and Samples

For optical excitation mid-infrared (MIR), terahertz and visible laser radiation was used. Most of the measurements were carried out at terahertz frequencies with photon energies less than the energy gap ε_g. Depending on the photon energy and QW band structure the MIR and THz radiation induce direct transitions between size quantized subbands or, at longer wavelength, Drude absorption. A pulsed TEA-CO_2 laser and a molecular THz laser [1, 38]

have been used as radiation sources in the spectral range between 9.2 μm and 496 μm.

Molecular THz is inexpensive and covers the terahertz spectral range with dense lying discrete lines. Depending on pumping, very high power levels are available also from compact designed laser systems. As pump sources CO_2 laser is utilized. The basic idea of the optically pumped molecular laser is to excite a vibrational-rotational transition of a molecule having a permanent electric dipole moment with the CO_2 laser in the mid-infrared and to obtain laser action in the terahertz range by purely rotational transitions. The principle of operation of such lasers was developed and used to achieve cw lasing by Chang and Bridges in 1969 [39], and in 1974 de Temple extended it to obtain pulsed laser operation [40]. Thousands of laser lines with wavelength from about 20 μm to 2 mm have been found until now covering the whole terahertz range. In Fig. 1 the spectrum of a set of discrete laser lines spread over the terahertz range is plotted. While there are many laser molecules, D_2O, NH3, and CH3F are used most frequently. All lines occur as single lines which is important for spectroscopic applications where multiline emission due to cascades of transitions must be avoided. Some experiments on photocurrents in the MIR have been carried out making use of the tunability of the free-electron laser "FELIX" [41]. For optical inter-band excitation a cw-Ti:sapphire lasers were used providing radiation with power $P \approx 100mW$.

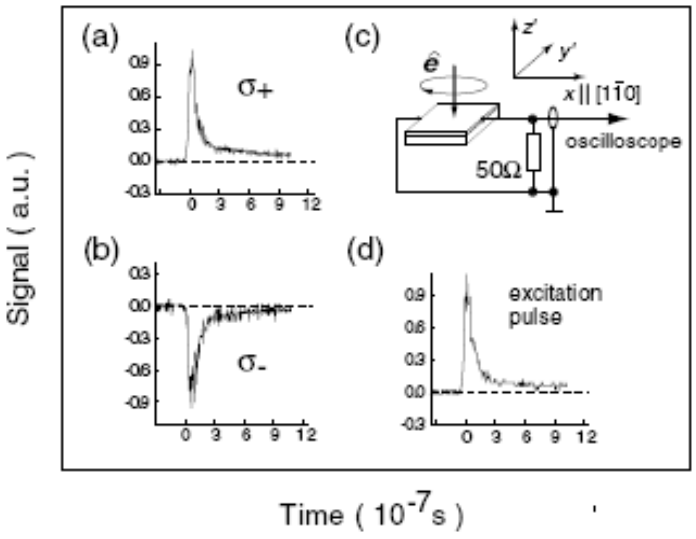

Fig. 2 Oscilloscope traces obtained for pulsed excitation of (113)-grown n-type GaAs QWs at λ = 10.6 μm and normal incidence. (a) and (b) show CPGE signals, (c) the measurement arrangement and (d) a signal pulse of a fast photon drag detector. For (001)-grown QWs oblique incidence was used in order to obtain helicity dependent current.

The circular polarization has been obtained using a Fresnel rhomb, ¸$\lambda/4$ plates, and a photoelastic modulator for MIR, THz and visible radiation, respectively. The helicity Pcirc of the incident light was varied from -1(left-handed circular, σ_-) to +1 (right-handed circular, σ_+)

according to $p_{circ} = \sin 2\varphi$, where the phase angle is the angle between the initial plane of polarization and the optical axis of the polarizer. Samples were studied in the temperature range of 4.2 K to 300 K. The photocurrent j_x was measured in the unbiased structures via the voltage drop across a $50\,\Omega$ load resistor in a closed circuit conguration (see Fig. 2c) [42]. For measurements in visible radiation modulation technique applying photoelastic modulator is frequently used.

The experiments were carried out on GaAs, InAs, asymmetric SiGe QWs, GaN, HgTe QWs and BeZn-MnSe QW structures belonging to two different classes of symmetry. Higher symmetric structures were (001)-oriented asymmetric QWs which corresponded to the point group C_{2v}. Structures of the lower symmetry class Cs were (113)-oriented and asymmetric (110)-oriented QWs. Samples of n- and p-type QWs with width Lw from 7 nm to 20 nm and free-carrier densities from 10^{11} cm^{-2} to $2 \bullet 10^{12}$ cm^{-2} were studied. Some experiments on the spin-galvanic effect required an external magnetic field. These measurements were performed at room temperature in a conventional electromagnet with the magnetic field up to 1 T and at low temperatures using a superconducting split-coil magnet.

3. Circular photogalvanic effect

The circular photogalvanic effect was independently predicted by Ivchenko and Pikus [22] and Belinicher [43]. It was first observed and studied in tellurium crystals by Asnin et al. [44], see also [2, 3, 45]. In tellurium the current arises due to spin splitting of the valence band edge at the boundary of the first Brillouin-zone (camel back"structure). While neither bulk zinc-blende materials like GaAs and related compounds nor bulk diamond crystals like Si and Ge allow this effect, in QW structures CPGE is possible due to a reduction of symmetry. CPGE in QWs was observed by Ganichev et al. applying terahertz radiation [12]. The CPGE appears due to the asymmetry of the momentum distribution of photoexcited carriers in homogeneous samples and be longs to the class of photogalvanic effects (for reviews see [2, 3, 45, 46]). The microscopic origin of this current is the conversion of photon angular momentum into directed motion of carriers. The data can be described by simple analytical expressions derived from a phenomeno-logical theory which shows that the effect can only be present in gyrotropic media.

3.1 Experiment: General Features

Illumination of QW structures by polarized radiation results in a current signal proportional to the helicity Pcirc [42]. The irradiated QW structure represents a current source wherein the current flows in the QW (see Fig. 2c). Figures 2a and 2b show measurements of the voltage drop across a 50 Ohm load resistor in response to 100 ns laser pulses at $\lambda = 76\,\mu m$. Signal traces are plotted for right-handed (a) and left-handed circular polarization (b), in comparison to a reference signal shown in Fig. 2d and obtained from a fast-photon drag detector [1, 2]. The width of the current pulses is about 100 ns which correspond to the THz laser pulses duration.

In (001)-oriented samples a helicity dependent signal s only observed under oblique incidence [12]. A variation of the angle of incidence in the incidence plane round normal incidence changes the sign of the current. For light propagating along〈110〉 direction the photocurrent flows perpendicular to the wave vector of the incident light (see Fig. 3a). For illumination along a cubic axis〈100〉both a transverse and a longitudinal CPGE current are detected [2]. In samples grown on a (113)-GaAs surface representing the lower symmetry class Cs, the CPGE has been observed also under normal incidence of radiation [12] as shown in Fig. 3b. This is in contrast to (001)-oriented samples and in accordance to the phenomenological theory of the CPGE for Cs. For normal incidence in this symmetry the current always flows along the [110]-direction perpendicular to the plane of mirror refection of the point group C_s.

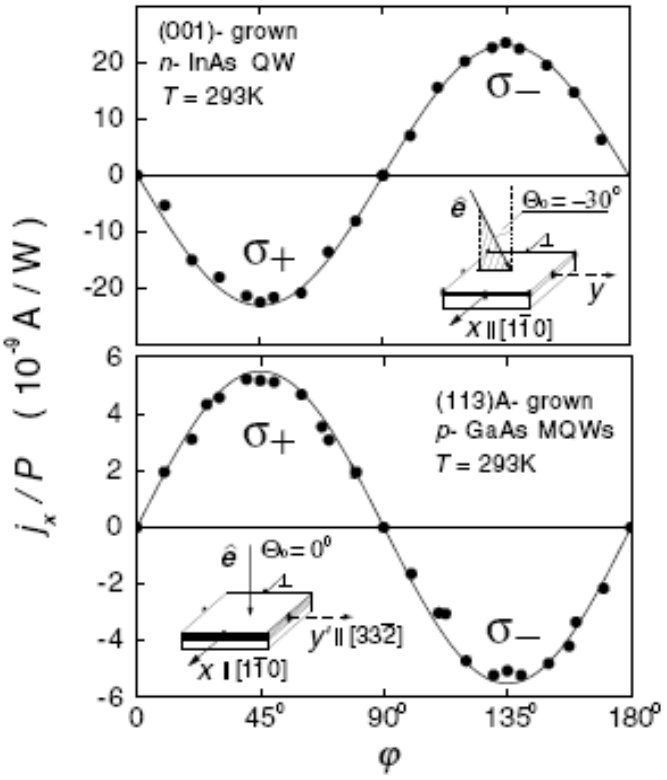

Fig. 3 Photocurrent in QWs normalized by the light power P as a function of the phase angle defning helicity. Measurements are presented for T = 293 K and ¸ λ = 76 um. (a)oblique incidence of radiation with an angle of incidence on (001)- grown QWs (symmetry class C2v). (b)normal incidence of radiation on (113)- grown QWs (symmetry class C_s). Full lines show ordinate scale fits after Eq. (2) and (3) for the top and lower panel, respectively. The insets show the geometry of the experiment.

3.2 **Phenomenology**

Phenomenologically the CPGE current j can be described as (see e.g. [3])

$$j_\lambda = \sum_\mu \gamma_{\lambda\mu} \lambda_\mu i(E \times E^*)_\mu \tag{1}$$

where γ is a pseudo-tensor, E is the complex amplitude of the radiation electric field, $i(E \times E^*)_u = \hat{e}_u E_0^2 P_{circ}$, E_0 and $\hat{e}$ are the electric field amplitude and the unit vector pointing in the direction of light propagation, respectively. In general, in addition to the CPGE current given in Eq. (1), two other photocurrents can be present simultaneously, namely the linear photogalvanic effect (LPGE) and the photon drag effect [1, 3]. Both effects were observed in low dimensional structures. These photocurrents are not changed in sign or amplitude if the polarization is switched from σ_+ to σ_- which allow to distinguish them from the CPGE. They do not require spin orientation and are outside the scope of the present investigation.

In the following we analyze Eq. (1) for symmetries relevant to experiment. Hereafter we use for (001)-grown QWs cartesian coordinates $x \| (1\bar{1}0)$, $y \| (110)$, $z \| (001)$ and for (113)-grown QWs the coordinates $x' = x \| (1\bar{1}0)$, $y' \| (33\bar{2})$, and $z' \| (113)$. For C_{2v} symmetry the photocurrent is given by

$$j_x = \gamma_{xy} e_y E_0^2 P_{circ} \qquad j_y = \gamma_{yx} e_x E_0^2 P_{circ} \tag{2}$$

If $\hat{e}$ is along $\langle 110 \rangle$ then the current flows normal to the light propagation direction. If the sample is irradiated with $\hat{e}$ parallel to h100i the current is neither parallel nor perpendicular to the light propagation direction. Another conclusion from Eq. (2) is that in QWs of C2v symmetry the photocurrent can only be induced under oblique incidence of radiation. For normal incidence $\hat{e}$ is parallel to [001] and hence the current vanishes. In contrast to this result in QWs of Cs symmetry a photocurrent also occurs for normal incidence of the radiation because the tensor γ has an additional component $\gamma_{xz'}$. The current here is given by

$$j_x = (\gamma_{xy'} e_{y'} + \gamma_{xy'} e_{z'}) E_0^2 P_{circ} \qquad j_{y'} = \gamma_{y'x} e_x E_0^2 P_{circ} \tag{3}$$

At normal incidence, $\hat{e}_x = \hat{e}_{y'} = 0$ and $\hat{e}_{z'} = 1$, the current in the QW flows along x, i.e. perpendicular to the mirror reflection plane. The dependence of the photocurrent on the angle of incidence θ_0 is determined by the value of the projection ^e on the x- (y-) axis (see Eqs (2)) or on the z'-axis (Eqs. (3)). The phenomenological picture outlined above perfectly describes the experimental observations [2].

3.3 **CPGE at Inter-Subband Transitions**

Microscopically a conversion of photon helicity into a spin photocurrent arises due to a removal of spin degeneracy in the k-space resulting in a shift of two spin subbands as sketched in Fig. 4. The band spin splitting k-linear terms in the effective Hamiltonian H= $\sum_{lm}\beta_{lm}\sigma_t k_m$ where *k* is the electron wave vector, σ_l are the Pauli spin matrices and β_{lm} are real coefficients. The coefficients β_{lm} form a pseudo-tensor subjected to the same symmetry restriction as the transposed pseudotensor γ The sources of k-linear terms are the bulk inversion asymmetry (BIA) also called the Dresselhau term [47] (including a possible interface inversion asymmetry [48]) and possibly a structural inversion asymmetry (SIA) usually called the Rashba term [9].

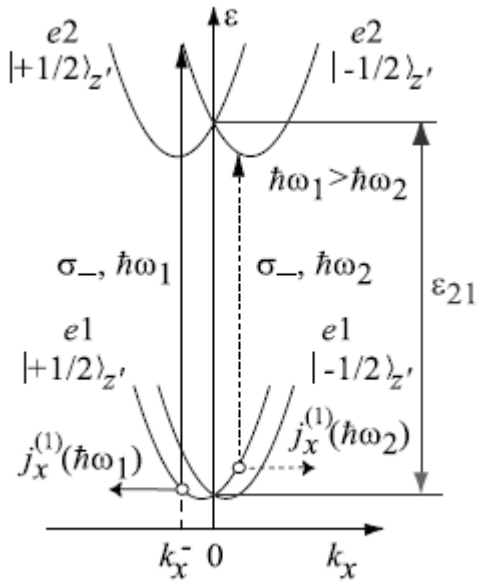

Fig. 4 Microscopic picture describing the origin of the circular photogalvanic current and its spectral inversion in C_s point group samples. The essential ingredient is the splitting of the conduction band due to k-linear terms. Left handed circularly polarized radiation σ_- induces direct spin-flip transitions (vertical arrows) from the e1 subband with s = 1/2 to the e2 subband with $s'=1/2$. As a result an unbalanced occupation of the k_x states occurs yielding a spin polarized photocurrent. For transitions with K_x^- lying left to the minimum of e1 (s = 1/2) subband the current indicated by j_x is negative. At smaller ω the transition occurs at a value of k_x on the right-hand side of the subband minimum, and the current reverses its sign.

The model of CPGE is most easily conceivable for inter-subband transitions from the

schematic band structure shown in Fig. 4 [49]. For the sake of simplicity we take into account a band structure consisting only of the two lowest conduction subband e1 and e2. In Fig. 4 we sketch direct transition between size quantized states in the conduction band for QWs of C_s symmetry. Due to selection rules optical transitions for monochromatic, say σ_+, radiation occur only at a fixed k_x^+ where the energy of the incident light matches the transition energy as is indicated by the arrow in Fig. 4. Therefore optical transitions induce an imbalance of momentum distribution in both subbands yielding an electric current in x direction with contributions from e1 and e2. As in n-type QWs the energy separation ε_{21} between e1 and e2 is typically larger than the energy of longitudinal optical phonons $\hbar w_{LO}$, the non-equilibrium distribution of electrons in e2 relaxes rapidly due to emission of phonons. As a result, the momentum relaxation time in e2 subband, $\tau_p^{(2)}$, is much less than $\tau_p^{(1)}$, the momentum relaxation time in e1 subband. Thus the current is mainly due to the photogenerated holes in the initial state of the resonant optical transition in the e1 subband.

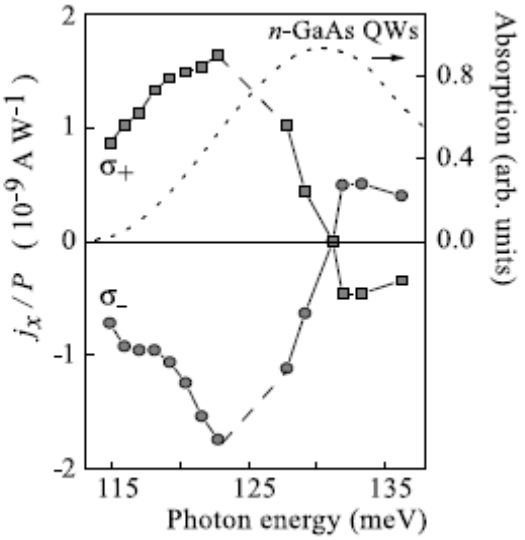

Fig. 5 Photocurrent in QWs normalized by the light power P as a function of the photon energy $\hbar w$. Measurements are presented for n-type(001)-grown GaAs/AlGaAs QWs of 8.2nm width at room temperature. Oblique incidence of σ_+ (squares) and σ_- (circles) circularly polarized radiation with an angle of incidence $\theta_0 = 20^o$ was used. The current j_x was measured perpendicular to the light incidence plane (y, z). The dotted line shows the absorption measurement using a Fourier transform infrared spectrometer. After [49].

The microscopic theory of CPGE for direct inter-subband transitions in n-type QWs for

both C_S and C_{2v} symmetry was developed in [49] with the result that the current is proportional to the derivative of the absorbance. For $\tau_p^{(2)}$ much less than $\tau_p^{(1)}$ it was shown that for C_S symmetry

$$j_x \sim \left(\beta_{yx}^{(2)} + \beta_{yx}^{(1)}\right)\left(\tau_p^{(1)} - \tau_p^{(2)}\right)\frac{d\eta_{12}(\hbar\omega)}{d\hbar\omega} IP_{circ}\hat{e}_{y,} \quad (4)$$

where $\beta_{yx}^{(1)}$ and $\beta_{yx}^{(2)}$ are components of β in the e1 and e2 subbands, respectively. The change of sign of the photocurrent with photon energy may be understand from the Fig. 4. It is seen that at large photon energy, $\hbar w > \varepsilon_{21}$, excitation occurs at positive κ_x resulting in a current j_x shown by arrow in Fig. 4. Decreasing of the photon frequency shifts the transition towards negative κ_x and reverses the current direction. Similar arguments hold for C_{2v} symmetry under oblique incidence.

Experimentally CPGE at resonant transitions was observed in n-type GaAs samples of QW widths from 8.2 to 8.6 nm. Direct optical transitions between e1 and e2 subband were excited applying MIR radiation of the CO_2 laser or free-electron laser "FELIX". A current signal proportional to the helicity has been observed at normal incidence in (113)-samples and at oblique incidence in (001)-oriented samples indicating the CPGE [49]. In Fig. 5 the data are presented for a (001)-grown n-GaAs QW of 8.2 nm width. It is seen that in direction x the current for both, σ_+ and σ_- radiation, changes sign at a frequency of the absorption peak. Experimental results shown in Fig. 5, in particular the sign inversion of the spectral behaviour of the current, are in a good agreement with microscopic theory developed in [49].

The CPGE at direct inter-subband transitions has also been observed in p-type QWs demonstrating spin orientation of holes (see Fig. 3b) [12, 32]. To achieve hh1-lh1 transitions in GaAs QWs THz radiation was applied. CPGE current has also been detected in artificially grown non-symmetric SiGe(001)-grown QWs being caused by the Rashba spin-orbit coupling due to a built-in potential gradient in the QWs [50].

3.4 CPGE at Drude Absorption

Now we consider indirect intra-subband transitions. This situation is usually realized in the THZ range where the photon energy is not high enough to excite direct inter-subband transitions. Due to energy and momentum conservation intra-subband transitions can only occur by absorption of a photon and simultaneous absorption or emission of a phonon. This process is described by virtual transitions involving intermediate states. It can be shown that

transitions via intermediate states within one and the same subband do not contribute to the spin photocurrent. However, spin selective indirect optical transitions excited by circularly polarized light can generate a spin current if virtual processes involve intermediate states in different subbands [12].

Optical absorption caused by indirect transitions in n-type samples have been obtained applying THz radiation covering the range of $76\,\mu m$ to $280\,\mu m$. The experiments were carried out on quantum wells based on GaAs [12, 51], InAs [12], semimagnetic ZnBeMnSe, HgTe and GaN [52]. The energy separation between e1 and e2 size-quantized subbands of those samples is much larger than the THZ photon energies used here. Therefore the absorption is caused by indirect intra-subband optical transitions. With illumination of (001)-grown QWs at oblique incidence of THZ radiation a current signal proportional to the helicity p_{circ} has been observed (see Fig. 3a) showing that Drude absorption of a 2D electron gas results in spin orientation and the CPGE. CPGE at intra-subband absorption was also observed in p-type samples at long wavelengths [42, 50, 51], where the photon energies are smaller than the energy separation between heavy-hole and light-hole subbands.

3.5 CPGE at Inter-Band Transitions

For direct optical transitions between the heavy-hole valence subband hh1 and conduction subband e1, the model circular PGE is very similar to inter-band transitions discussed above [12]. The circular PGE at interband absorption was observed in GaAs-, InAs- and GaN-based QW structures [53-56]. Investigation of spectral response of the circular photogalvanic current observed in (001)-grown $In_xGa_{1-x}As/InAlAs$ QW structures [55] demonstrated that the photocurrent spectral contour exhibits a change in sign, in a qualitative agreement with the theoretical prediction [57].

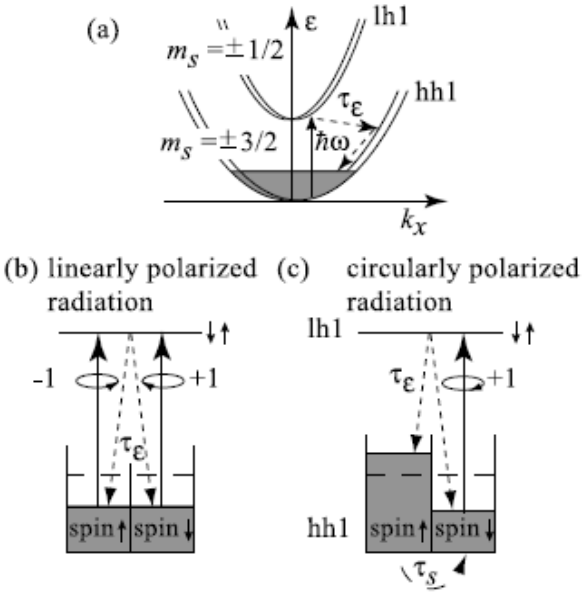

Fig. 6 (a)-(c) Microscopic picture of spin sensitive bleaching: Direct hh1-lh1 optical transitions (a) and process of bleaching for two polarizations, linear (b) and circular (c). Dashed arrows indicate energy (τ_ε) and spin (τ_s) relaxation.

3.6 Spin-sensitive bleaching

Application of high THz radiation intensities results in saturation (bleaching) of PGE. This effect was observed for direct intersubband transitions in p-type GaAs QWs and gave an experimental access to spin relaxation times [31, 32]. The method is based on the difference in nonlinear behavior of CPGE and LPGE. Both currents are proportional to absorption and their nonlinear behavior reflects the nonlinearity of absorbance.

Spin sensitive bleaching can be analyzed in terms of a simple model taking into account both optical excitation and nonradiative relaxation processes. Excitation with THz radiation results in direct transitions between heavy-hole (hh1) and light-hole (lh1) subbands (Fig. 6a). This process depopulates and populates selectively spin states in the hh1 and lh1 subbands. The absorption is proportional to the difference of populations of the initial and final states. At high intensities the absorption decreases since the photoexcitation rate becomes comparable to the nonradiative relaxation rate to the initial state. Absorption of linearly polarized light is not spin selective and the saturation is controlled by energy relaxation (see Fig. 6b). In contrast, absorption of circularly polarized light is spin selective due to selection rules, and only one type of spin is excited, Fig. 6c. Note that during energy relaxation the hot holes lose their photoinduced orientation due to rapid relaxation so that the spin orientation occurs only within the bottom of the hh1 subband. Thus the absorption bleaching of circularly polarized radiation is governed by energy relaxation of photoexcited carriers and spin relaxation within the subband hh1. These processes are characterized by energy and spin relaxation times, τ_ε and τ_s, respectively. If τ_s is longer than τ_ε the bleaching of absorption becomes spin sensitive and the saturation intensity of circularly polarized radiation drops below the value of linear polarization.

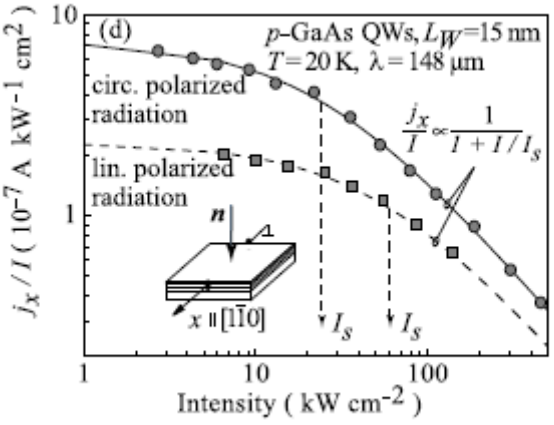

Fig. 7 Circular (squares) and linear PGE (circles) currents j_x normalized by the intensity as a function of the intensity for circularly and linearly polarized radiation. The inset shows the geometry of the experiment. The data are fitted to $j_x = I \propto 1/(1 + I/I_s)$ with one parameter I_s for each state of polarization. Data are given for (113)-grown samples after [31].

Bleaching of absorption with increasing the intensity of linearly polarized light is described phenomenologically by the function $\eta(I) = \eta_0 = (1 + I/I_{se})$, where $\eta_0 = \eta(I \to 0)$ and I_{se} is the characteristic saturation intensity controlled by energy relaxation of holes. Since the LPGE current, j_{LPGE}, induced by the linearly polarized light is proportional to ηI, one has

$$\frac{j_{LPGE}}{I} \propto \frac{1}{1+I/I_{se}} \tag{5}$$

The circular photogalvanic current j_{LPGE} induced by the circularly polarized radiation is proportional to the degree of hole spin polarization and given by [31]

$$\frac{j_{LPGE}}{I} \propto \frac{1}{1+I(I_{se}^{-1}+I_{ss}^{-1})} \tag{6}$$

where $I_{ss} = p_s \hbar\omega/(\eta_0 \tau_s)$, p_s is the 2D hole density.

The measurements shown in Fig. 7 indicate that the photocurrent j_x at a low power level depends linearly on the light intensity and gradually saturates with increasing intensity, $j_x = I \propto 1/(1 + I/I_s)$, where I_s is the saturation parameter. One can see from Fig. 7 that the measured saturation intensity for circular polarized radiation is smaller than that for linearly polarized light.Using the measured values of I_s and Eqs. (5) and (6) one can estimate the parameter I_{ss} and even the time τ_s [31, 32].

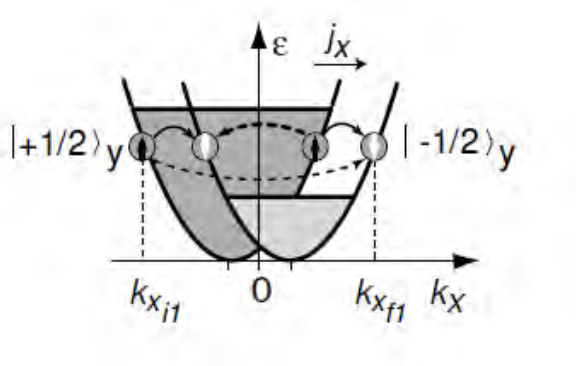

Fig. 8 Microscopic origin of the spin-galvanic current in the presence of κ-linear terms in the electron Hamiltonian.

4. Spin-Galvanic Effectt

Spin photocurrents described so far involved the asym metry of the momentum distribution of photoexcited carriers, i.e. the CPGE. After momentum relaxation of the photoexcited carriers the CPGE vanishes, however, aspin orientation may still be present if the spin relaxation time is longer than the momentum relaxation time. In such a case an asymmetry of spin-flip scattering of non-equilibrium spin polarized carriers may contribute to the current. This current is caused by the spin-galvanic effect and in general it does not require photoexcitation .

4.1 **Phenomenology**

The SGE is due to spin relaxation of a uniform nonequilibrium spin polarization in gyrotropic QWs [13].Phenomenologically, an electric current can be linked to the electron's averaged spin polarization S by

$$j_\alpha = \sum_\gamma Q_{\alpha\gamma} S_\gamma \tag{7}$$

Like in the case of CPGE here we have a pseudo-tensor Q with the same symmetry restrictions like γ. For C_{2v} symmetry of (001)-grown QWs only two linearly independent components, Q_{xy} and Q_{yx}, may be non-zero yielding

$$j_x = Q_{xy} S_y , \quad j_y = Q_{yx} S_x . \tag{8}$$

Hence, SGE current needs a spin component lying in the plane of QWs. In QWs of C_s symmetry an additional tensor component $Q_{xz'}$ is non-zero and the SGE may becaused by spins oriented normally to the plane of QW.

4.2 **Microscopic Model**

Microscopically, the spin-galvanic effect is caused by asymmetric spin-flip relaxation of spin polarized electrons in systems with k-linear contributions to the effective Hamiltonian [13]. Fig. 8 sketches the electron energy spectrum along k_x with the spin dependent term $\beta_{yx}\sigma_y\kappa_x$. Spin orientation in y-direction causes the unbalanced population in the subbands. The current flow is caused by k-dependent spin-flip relaxation processes.Spins

oriented in y-direction are scattered along k_x from the higher filled, e.g. spin-up subband, $|+1/2\rangle_y$, to the less filled spin-down subband, $|-1/2\rangle_y$. Four quantitatively different spin-flip scattering events exist and are sketched in Fig. 8 by bent arrows. The spin-flip scattering rate depends on the values of the wavevectors of the initial and the final states, respectively [58]. Two scat tering processes shown by broken arrows are inequivalent and generate an asymmetric carrier distribution around the subband minima in both subbands. This asymmetric population results in a current flow along the x-direction. The uniformity of spin polarization in space is preserved during the scattering processes. Therefore the spin-galvanic effect differs from other experiments where the spin current is caused by inhomogeneities [59-61]. Up to now the spin-galvanic effect has been recorded at optical spin orientation caused by inter-band, inter-subband,as well as intra-subband transitions [13, 14]. The microscopic theory of the SGE is developed in [14, 62].

4.3 **Experiments on spin-galvanic effect**

The spin-galvanic effect can be investigated by pure optical spin orientation due to absorption of circularly polarized radiation in QWs. Such optical excitation results in a spin polarization which, at proper orientation of the electron spins, causes the SGE. However, because of the tensor equivalence, the spin-galvanic current induced by circularly polarized light always occurs simultaneously with the CPGE. Nevertheless, microscopically these two effects are definitely inequivalent. Indeed, the SGE is caused by asymmetric spin-flip scattering of spin polarized carriers and determined by the spin relaxation processes. If spin relaxation is absent the SGE vanishes.In contrast, the CPGE is a result of selective photoexcitation of carriers in the k-space with circularly polarized light due to optical selection rules, it is independent of the spin relaxation if $\tau_s \gg \tau_p$. It has also been recently shown, that at inter-subband transitions the SGE may be separated from CPGE making use of the spectral behaviour at resonance [14].

Another possibility to investigate the spin-galvanic effect without contributions of the CPGE to the current has been introduced in [13]. The spin polarization was obtained by absorption of circularly polarized radiation at normal incidence on (001)-grown QWs as depicted in the inset of Fig. 9. For normal incidence the CPGE as well as the spin-galvanic effect vanish because $\hat{e}_x = \hat{e}_y = 0$ (see Eqs. (2)) and $S_x = S_y = 0$ (see Eqs.(8)), respectively. Thus, we have a spin orientation along the z coordinate but no spin photocurrent.

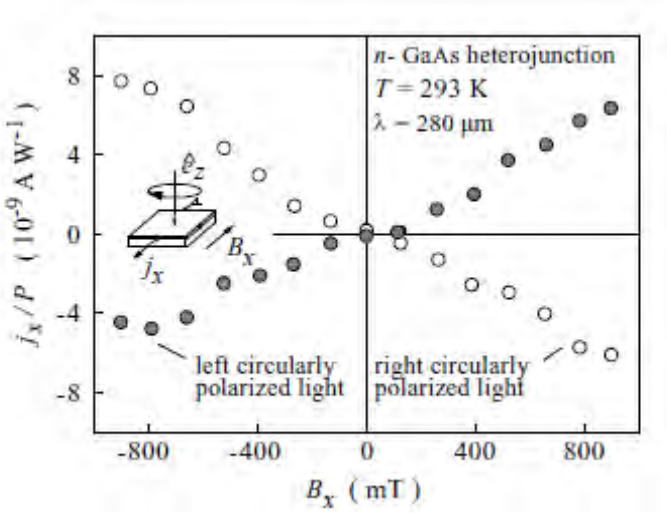

Fig. 9 Spin-galvanic current J_x normalized by P as a function of magnetic field B at room temperature. SGE is achieved by intra-subband transitions within the e1 conduction subband by excitation with radiation of $\lambda = 280 \mu m$ wave-length. Results are plotted for an (001)-grown GaAs single heterojunction at room temperature. The inset shows the geometry of the experiment where $\hat{e}_z$ indicates the direction of the incoming light. Data are given after [2].

To obtain an in-plane component of the spins, necessary for the spin-galvanic effect, a magnetic field $B \| x$ has been applied. Due to Larmor precession a non-equilibrium spin polarization S_y is induced being

$$S_y = -\frac{w_L \tau_{S\perp}}{1+(\omega_L \tau_s)^2} S_{0z} \tag{9}$$

where $\tau_s = \sqrt{\tau_s \| \tau_{s\perp}}, \tau_{s\perp}, \tau_{s\perp}$ are the longitudinal and transverse electron spin relaxation times, w_L is the Larmor frequency. The denominator in Eq. (9) yielding the decay of S_y for $\omega_L \tau_s > 1$ is well known from the Hanle effect [10].

Both, for visible and THz radiation, a current due to SGE has been observed for all (001)-grown n-type GaAs and InAs samples after applying an in-plane magnetic field [13, 36]. For low magnetic fields B where $\omega_L \tau_s < 1$ holds, the current increases linearly as expected from Eqs. (8) and (9). The polarity of the current depends on the direction of the excited spins determined by the radiation helicity and the direction of the applied magnetic field. For

magnetic field applied along <110> the current flows along the magnetic field. For $B \| <100>$ both the transverse and the longitudinal effects are observed [2].For higher magnetic fields the current assumes a maxi-mum and decreases upon further increase of B [13]. This drop of the current is ascribed to the Hanle effect [10].The experimental data are well described by Eqs. (8) and (9). The observation of the Hanle effect demonstrates that free carrier intra-subband transitions can polarize the spins of electron systems. The measurements allow to obtain the spin relaxation time τ_s from the peak position of the photocurrent where $\omega_L \tau_s = 1$ holds [13].

In the experiments described above a magnetic field was used for re-orientation of an optically generated spin polarization. The SGE can also be occur at optical excitation only, without application of an external magneticfield. The necessary in-plane component of the spin polarization can be obtained by oblique incidence of the exciting circularly polarized radiation but, as addressed above, in this case the CPGE may also occur interfering with the SGE. However, a pure SGE may be obtained at inter-subband transitions in n-type GaAs QWs [14].The spin orientation is generated by spin-selective optical excitation followed by spin-non-specific thermalization. The magnitude of the spin polarization and hence the current depends on the initial absorption strength but not on the k of transition. Thus the spin-galvanic current is proportional to the absorbance [36]. In contrast, as shown above the spectrum of CPGE changes sign and vanishes in the center of resonance (see Fig. 5 and [49]). Therefore, if a helicity dependent current is present in the center of the resonance it must be attributed to the SGE. Such a behaviour has been observed in GaAs QW structures at resonance excitation with MIR radiation demonstrating the SGE at pure optical excitation [14]. Experiments have been carried out making use of the spectral tunability of the free electron laser "FELIX" [41].

4.4 Inverse spin-galvanic effect

The effect inverse to the spin-galvanic effect is the electron spin polarization generated by a charge current j. First it was predicted in [16] and observed in bulk tellurium[63]. Aronov, Lyanda-Geller[64],Edelstein[65]and Vas'ko [66] demonstrated that spin orientation by current is also possible in QW systems. This study was extended in Refs. [67-72]. Most recently the first direct experimental proofs of this effect were obtained in semiconductor QWs [19, 20] as well as in strained bulk material [21]. At present inverse spin-galvanic effect in low-dimensional structures has been observed applying various experimental techniques, comprising transmission of polarized THz-radiation, polarized luminescence and space resolved Faraday rotation [19-21, 55, 73-75].

Phenomenologically, the averaged nonequilibrium free carrier spin S is linked to j by

$$S_\mu = R_{\mu\lambda j\lambda} \cdot \tag{10}$$

Microscopic model of the current induce spin orientation is similar to that of the spin galvanic effect presented above. Following [19] we sketch in Fig. 10b this model for (113)-grown

p-type QWs. Due to k-linear terms in the effective Hamiltonian the parabolic energy band splits into two parabolic subbands of opposite spin directions, $s_{z'} = 3/2$ and $s_{z'} = -3/2$, with minima symmetrically shifted in the k-space along the k_x axis from the point $k = 0$ into the points $\pm k_0$, where $k_0 = m_c \beta_{z'x} / \hbar^2$. The

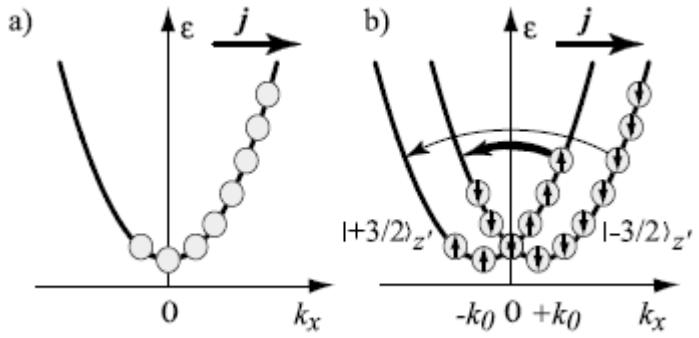

Fig.10 Comparison of current flow in (a) spin-degenerate and (b) spin-split subbands. (a) Hole distribution at a stationary current flow due to acceleration in an electric field and momentum relaxation. (b) Spin polarization due to spinflip scattering. Here only $\beta_{z'x}\sigma_{z'}k_x$ term is taken into account in the Hamiltonian which splits the valence subband into two parabolas with spin-up $|+3/2\rangle_{z'}$ and spin-down $|-3/2\rangle_{z'}$ in the z'-direction. Biasing along the x-direction causes an asymmetric in k-space occupation of both parabolas. After[19].

The corresponding dispersion is sketched in Fig. 10b. In the presence of an in-plane electric field $F \| x$ the distribution of carriers in the k-space gets shifted yielding an electric current. Until the spin relaxation is switched off the spin branches are equally populated and equally contribute to the current. Due to the band splitting, spinfip relaxation processes $\pm 3/2 \rightarrow \mp 3/2$ are different because of the difference in quasi-momentum transfer from initial to final states. In Fig. 10b the k-dependent spinflip scattering processes are indicated by arrows of different lengths and thicknesses. As a consequence different amounts of spin-up and spin-down carriers contribute to the spin-flip transitions causing a stationary spin orientation. Thus, in this picture we assume that the origin of the current induced spin orientation is, as sketched in Fig. 10b, exclusively due to scattering and hence dominated by the Elliott-Yafet spin relaxation processes.

5. CPGE versus spin-galvanic effect

The circular photogalvanic effect and the spin-galvanic effect have in common that the current flow is driven by an asymmetric distribution of carriers in k-space in systems with lifted spin degeneracy due to k-linear terms in the Hamiltonian. The crucial difference between both effects is, that the SGE may be caused by any means of spin injection, while the CPGE needs optical excitation with circularly polarized radiation. Even if the SGE is achieved by optical spin orientation, as discussed here, the microscopic mechanisms are

different. The SGE is caused by asymmetric spin-flip scattering of spin polarized carriers and it is determined by the process of spin relaxation (see Fig. 8). If spin relaxation is absent, the spin-galvanic current vanishes. In contrast, the CPGE is the result of selective photoexcitation of carriers in k-space with circularly polarized light due to optical selection rules and depends on momentum relaxation (seeFig.4). In some optical experiments the observed photocurrent may represent a sum of both effects. For example, if we irradiate an (001)-oriented QW at oblique incidence of circularly polarized radiation, we obtain both selective photoexcitation of carriers in k-space determined by momentum relaxation and the spin-galvanic effect due to an in-plane component of non-equilibrium spin polarization. Thus both effects contribute to the current occurring in the plane of the QW. The two mechanisms can be distinguished by time resolved measurements because usually momentum relaxation time and spin relaxation time are different.

6. **Application of spin photocurrents**

Spin photocurrents provide an experimental access to spin properties of QWs and are also implied for detection of helicity of THz radiation with picosecond time resolution [34]. Spin photocurrents are applied to investtigate spin relaxation times at monopolar spin orientation where only one type of charge carriers is involved in the excitation-relaxation process [2]. This condition is close to that of electrical spin injection in semiconductors. Two methods based on nonlinearity of spin photocurrents allowing to measure spin sensitive bleaching [31, 32] and the Hanle effect in the spin-galvanic current [13] were already introduced above.

A further important application of both SGE and CPGE was addressed by Ganichev et al. in [29, 30]. It is demonstrated that angular dependent measurements of spin photocurrents allow to separate Dresselhaus and Rashba terms. The relative strength of these terms is of importance because it is directly linked to the manipulation of the spin of charge carriers in semiconductors, one of the key problems in the field of spintronics. Spin polarization may be tuned by means of the Rashba spin-orbit coupling in QWs. In addition to the Rashba coupling, caused by structural inversion asymmetry, also a Dresselhaus type of coupling, caused by a lack of inversion symmetry in the host material, contributes to spin-splitting. In C_{2v} symmetry these terms are given by symmetric and anti-symmetric tensor components $\beta_{BIA} = 1/2(\beta_{xy} + \beta_{yx})$ and $\beta_{SIA} = 1/2(\beta_{xy} - \beta_{yx})$. Dresselhaus term β_{SIA} and Rashba term β_{SIA} result from bulk inversion asymmetry (BIA) and from structural inversion asymmetry (SIA), respectively.

Both, Rashba and Dresselhaus couplings, result in spin-splitting of the band and give rise to a variety of spin dependent phenomena which allow to evaluate the magnitude of the total spin splitting of electron subbands. However, usually it is not possible to extract the rela tive strengths of Rashba and resselhaus terms in the spin-orbit coupling. In obtaining the Rashba coefficient, the Dresselhaus contribution is normally neglected. At the same time, Dresselhaus and Rashba terms can interfere in such a way that macroscopic effects vanish though the individual terms are large [58, 76]. For example, both terms can cancel each other resulting in

a vanishing spin splitting in certain k-space directions [2]. This cancellation leads to the disappearance of an antilocalization [77], the absence of spin relaxation in specific crystallographic directions [58, 78], and the lack of Shubnikov-de Haas beating [76]. In [79] the importance of both Rashba and Dresselhaus terms was pointed out: tuning β_{SIA} such that $\beta_{SIA} = \beta_{BIA}$ holds, allows to build a non-ballistic spin field-effect transistor.

By mapping the magnitude of the spin photocurrent in the plane of a QW the ratio of both terms can directly be determined from experiment and does not relay on theoretically obtained quantities [29]. Indeed, the SGE is driven by the electron in-plane average spin $S_{||}$ according to [29]:

$$j_{SGE} \propto \begin{pmatrix} \beta_{BIA} - \beta_{SIA} \\ \beta_{SIA} - \beta_{BIA} \end{pmatrix} S_{||} \tag{11}$$

if $S_{||}$ is aligned along one of the cubic axes. Therefore, the SGE j_{SGE} consists of Rashba and Dresselhaus coupling induced currents, j_R R and j_D. Their magnitudes are $j_R \propto \beta_{SIA} \left| S_{||} \right|, j_D \propto \beta_{SIA} \left| S_{||} \right|$ and their ratio is

$$j_R / j_D = \beta_{SIA} / \beta_{BIA}. \tag{12}$$

To obtain the Rashba- and Dresselhaus contributions the spin-galvanic effect is measured for a fixed orientation of $S_{||}$ for various in-plane directions. Evaluating measurements yields immediately the ratio between Rashba and Dresselhaus terms. Three directions of spin population $S_{||}$ are particularly suited to extract the ratio between Rashba and Dresselhaus terms. In one of them the spin polarization $S_{||}$ is set along [100]. Then it follows from Eq. (11) that the currents along the [100]direction and [010]-direction are equal to j_D and j_R, respectively. The ratio of Rashba and Dresselhaus currents can be directly read off from these current strengths. In InAs structure described in [29] the value obtained by this method in is $j_R / j_D = \beta_{SIA} / \beta_{BIA}$ = 2.1 being in good agreement to theoretical results [80] which predict a dominating Rashba spin-orbit coupling for InAs QWs. The method was also used for investigation of Rashba/Dresselhaus spin-splitting in GaAs heterostructures where spin relaxation is controlled by Dyakonov-Perel mechanism [30]. These experiments demonstrate that growth of structures with various delta-doping layer position accompanied by experiments on spin-galvanic effect makes possible a controllable variation of the structure inversion asymmetry and preparation of samples with equal Rashba and Dresselhaus constants or with a zero Rashba constant.

7. **Summary**

A non-equilibrium uniform spin polarization obtained by optical orientation drives an electric current in QWs if they belong to a gyrotropic crystal class. Two different microscopic mechanisms of spin photocurrents can be distinguished, the CPGE and the spin-galvanic effect.In the first effect the coupling of the helicity of light to spin polarized final states with a net linear momentum is caused by selection rules together with band splitting in k-space. The current flow in the second effect is driven by asymmetric spin relaxation of a homogeneous nonequilibrium spin polarization. Investigation of both effects provides a deeper insight in the spin-dependent microscopic processes.

Acknowledgement

Financial support by the DFG is gratefully acknowledged.

References

[1] S. D. Ganichev and W. Prettl, “Intense Terahertz Excitation of Semiconductors”, Oxford Univ. Press, (2006).

[2] S.D. Ganichev, and W. Prettl, topical review, *J. Phys.: Condens. Matter*, 15, R935, (2003).

[3] E.L. Ivchenko, “Optical Spectroscopy of Semiconductor Nanostructures”, Alpha Science Int., Harrow, UK, (2005).

[4] I. Zutic, J. Fabian, and S. Das-Sarma, *Rev. Modern Phys.*76, 323, (2004).

[5] “Concepts in Spin Electronics”, eds. S. Maekawa, OxfordUniv. Press, Oxford, (2006).

[6] J. Fabian, A. Matos-Abiague, C. Ertler, P. Stano, I. Zutic, “Semiconductor Spintronics”, tutorial review, *Acta Physica Slovaca*, 57, 565, (2007) (arXiv:0711.1461).

[7] R. Winkler, “Spin-dependent transport of carriers in semiconductors in Handbook of Magnetism and Advanced Magnetic Materials”, edited by H. Kronmller and S. Parkin, Wiley, Chichester, V, 2830, (2007) (arXiv:cond-mat/0605390).

[8] D.D. Awschalom and M.E. Flatt, *Nature Physics*, 3, 153, (2007).

[9] Y.A. Bychkov, and E.I. Rashba, *Pis'ma ZhETF*, 39, 66, (1984) [Sov. *JETP Lett*., 39, 78, (1984)].

[10] Optical orientation, F. Meier, and B.P. Zakharchenya, Eds. Elsevier Science Publ., Amsterdam, (1984).

[11] The gyrotropic point group symmetry makes no difference between components of axial and polar vectors.

[12] S.D. Ganichev, E. L. Ivchenko, S.N. Danilov, J. Eroms, W. Wegscheider, D. Weiss, and W. Prettl, *Phys. Rev. Lett.*, 86, 4358, (2001).

[13] S.D. Ganichev, E.L. Ivchenko, V.V. Bel'kov, S.A. Tarasenko, M. Sollinger, D. Weiss, W. Wegscheider, and W. Prettl, *Nature* (London), 417, 153, (2002).

[14] S. D. Ganichev, Petra Schneider, V. V. Bel'kov, E. L. Ivchenko, S. A. Tarasenko, W. Wegscheider, D.Weiss, D. Schuh, D. G. Clarke, M. Merrick, B. N. Mur-din, P. Murzyn, P. J. Phillips, C. R. Pidgeon, E. V. Beregulin, and W. Prettl, *Phys. Rev. B. Rapid Communic.*, 68, 081302, (2003).

[15] W. Weber, S. Seidl, V.V. Bel'kov, L.E. Golub, E.L. Ivchenko, W. Prettl, Z.D. Kvon, Hyun-Ick Cho and Jung-Hee Lee and S.D. Ganichev, *Solid. State Comm.*, 145, 56, (2007).

[16] E.L. Ivchenko and G.E. Pikus, *Pisma Zh. Eksp. Teor. Fiz.*, 27, 640, (1978) [*JETP Lett.*, 27, 604, (1978)].

[17] A.G. Aronov, and Yu. B. Lyanda-Geller, *Pis'ma ZhETP*, 50, 398, (1989) [Sov. *JETP Lett.*, 50, 431, (1990)].

[18] V.M. Edelstein, *Solid State Comm.*, 73, 233, (1990).

[19] S.D. Ganichev, S.N. Danilov, Petra Schneider, V.V. Bel'kov, L.E. Golub, W. Wegscheider, D. Weiss, and W. Prettl, cond-mat/0403641, (2004), see also J. Magn. and Magn. Materials 300, 127, (2006).

[20] A.Yu. Silov, P.A. Blajnov, J.H. Wolter, R. Hey, K.H. Ploog, and N.S. Averkiev, *Appl. Phys. Lett.*, 85, 5929, (2004).

[21] Y.K. Kato, R.C. Myers, A.C. Gossard, and D.D. Awschalom, *Phys. Rev. Lett.*, 93, 176601, (2004).

[22] E.L. Ivchenko and G.E. Pikus, *Pis'ma Zh. Eksp. Teor. Fiz.*, 27, 640, (1978) [*JETP Lett.*, 27, 604, (1978)].

[23] E.L. Ivchenko and G.E. Pikus, *Izv. Akad. Nauk SSSR* (ser. fiz.), 47, 2369, (1983) [Bull. Acad. Sci. USSR, *Phys. Ser*., 47, 81, (1983)].

[24] V.V. Bel'kov, S.D. Ganichev, E.L. Ivchenko, S.A. Tarasenko, W. Weber, S. Giglberger, M. Olteanu, P. Tranitz, S.N. Danilov, Petra Schneider, W. Wegscheider, D. Weiss, and W. Prettl, *J. Phys. C: Condens. Matter*.,17, 3405, (2005).

[25] S.D. Ganichev, V.V. Bel'kov, S.A. Tarasenko, S.N. Danilov, S. Giglberger, Ch. Hoffmann, E.L. Ivchenko, D. Weiss, W. Wegscheider, Ch. Gerl, D. Schuh, J. Stahl, J.De Boeck, G. Borghs, andW. Prettl, *Nature Physics*, 2, 609, (2006).

[26] S.D. Ganichev, S.N. Danilov, V.V. Bel'kov, S. Giglberger, S.A. Tarasenko, E.L. Ivchenko, D. Weiss, W. Jantsch, F. SchÄa²er, D. Gruber, and W. Prettl, *Phys. Rev.*, B 75, 155317, (2007).

[27] R. Winkler, “Spin-Orbit Coupling Effects in Two Dimensional Electron and Hole Systems”, in Springer Tracts in *Modern Physics* ,Vol.191, Springer, Berlin, (2003).

[28] W. Zawadzki, and P. Pfeffer, Semicond. *Sci. Technol*. 19, R1, (2004).

[29] S.D. Ganichev, V.V. Bel'kov, L.E. Golub, E.L. Ivchenko, Petra Schneider, S. Giglberger, J. Eroms, J.

eBoeck, G. Borghs, W. Wegscheider, D. Weiss, and W. *Prettl, Phys. Rev. Lett.*, 92, 256601, (2004).

[30] S. Giglberger, L.E. Golub, V.V. Bel'kov, S.N. Danilov, D. Schuh, Ch. Gerl, F. Rohl¯ng, J. Stahl, W. egschei der, D. Weiss, W. Prettl, and S.D. Ganichev, *Phys. Rev.*, B 75, 035327, (2007).

[31] S.D. Ganichev, S.N. Danilov, V.V. Bel'kov, E.L. Ivchenko, M. Bichler, W. Wegscheider, D. Weiss, and W. Prettl, *Phys. Rev. Lett.*, 88, 057401-1, (2002).

[32] P. Schneider, J. Kainz, S.D. Ganichev, V.V. Bel'kov, S.N. Danilov, M.M. Glazov, L.E. Golub, U. RÄossler, W. Wegscheider, D. Weiss, D. Schuh, and W. Prettl, *J. Appl. Phys.*, 96, 420, (2004).

[33] V.V. Bel'kov, P. Olbrich, S.A. Tarasenko, D. Schuh, W. Wegscheider, T. Korn, C. SchÄuller, D. Weiss, W. Prettl, and S.D. Ganichev, arXiv:0712.1704v1.

[34] S.D. Ganichev, J. Kiermaier, W. Weber, S.N. Danilov, D. Schuh, Ch. Gerl, W. Wegscheider, D. Bougeard, G. Abstreiter, and W. Prettl, *Appl. Phys. Lett.*, 91, 091101, (2007).

[35] S.A. Tarasenko, E.L. Ivchenko, V.V. Bel'kov, S.D. Ganichev, D. Schowalter, Petra Schneider, M. Sollinger, W. Prettl, V.M. Ustinov, A.E. Zhukov, and L. E. Vorobjev, cond-mat/0301393, (2003).

[36] S.A. Tarasenko, E.L. Ivchenko, V.V. Bel'kov, S.D. Ganichev, D. Schowalter, Petra Schneider, M. Sollinger, and W. Prettl, V.M. Ustinov, A.E. Zhukov, and L.E. Vorobjev, *Journal of Supercond.: Incorporating novel Magn.*, 16, 419, (2003).

[37] E.L. Ivchenko and S.A. Tarasenko, *Zh. Eksp. Teor. Fiz.*, 126, 476, (2004) [*JETP*, 99, 379, (2004)].

[38] S.D. Ganichev, I.N. Yassievich, and W. Prettl, *J. Phys.: Condens. Matter*, 14, R1263, (2002).

[39] T.Y. Chang and T.J. Bridges, *Optics Commun.*, 1, 423,(1970).

[40] T.A. DeTemple, “Pulsed Optically Pumped Far Infrared Lasers, in Infrared and Millimeter Waves”, Vol. 1, Sources of Radiation, ed. K.J. Button, Academic Press, New York, 129-153, (1979).

[41] G.M.H. Knippels, X. Yan, A.M. MacLeod, W.A. Gillespie, M. Yasumoto, D. Oepts and A.F.G. van der Meer, *Phys. Rev. Lett.*, 83, 1578, (1999).

[42] S.D. Ganichev, E.L. Ivchenko, H. Ketterl, W. Prettl, and L.E. Vorobjev, *Appl. Phys. Lett.*, 77, 3146, (2000).

[43] V.I. Belinicher, *Phys. Lett.*, A 66, 213, (1978).

[44] V.M. Asnin, A.A. Bakun, A.M. Danishevskii, E.L. Ivchenko, G.E. Pikus, A.A. Rogachev, *Pis'ma Zh. Eksp. Teor. Fiz.*, 28, 80, (1978) [*JETP Lett.*, 28, 74, (1978)].

[45] B.I. Sturman, and V.M. Fridkin, “The Photovoltaic and Photorefractive Effects in Non-Centrosymmetric Materials”, Gordon and Breach Science Publishers, New York, (1992).

[46] E.L. Ivchenko, and G.E. Pikus, “Superlattices and Other Heterostructures”, Symmetry and Optical Phenomena, Springer, Berlin, (1997).

[47] M.I. D'yakonov, and V.Yu. Kachorovskii, *Fiz. Tekh. Poluprov.*, 20, 178, (1986) [Sov. *Phys. Semicond.*, 20, 110, (1986)].

[48] O. Krebs, P. Voisin, *Phys. Rev. Lett.*, 77, 1829, (1996).

[49] S. D. Ganichev, V. V. Bel'kov, Petra Schneider, E. L. Ivchenko, S. A. Tarasenko, D. Schuh, W. Wegscheider, D. Weiss, and W. Prettl, *Phys. Rev.*, B 68, 035319, (2003).

[50] S.D. Ganichev, U. RÄossler, W. Prettl, E.L. Ivchenko, V.V. Bel'kov, R. Neumann, K. Brunner, and G. Bstreiter, *Phys. Rev.*, B 66, 75328, (2002).

[51] S.D. Ganichev, E.L. Ivchenko, and W. Prettl, *Physica*, E 14, 166, (2002).

[52] W.Weber, S.D. Ganichev, Z.D. Kvon, V.V. Bel'kov, L.E. Golub, S.N. Danilov, D. Weiss, W. Prettl, Hyun-Ick Cho, and Jung-Hee Lee, *Appl. Phys. Lett.*, 87, 262106, (2005)

[53] V.V. Bel'kov, S.D. Ganichev, Petra Schneider, C. Back, M. Oestreich, J. Rudolph, D. HÄagele, L.E. Golub, W. Wegscheider, and W. Prettl, *Solid State Commun.*, 128, 283, (2003).

[54] M. Bieler, N. Laman, H.M. van Driel, and A.L. Smirl, *Appl. Phys. Lett.*, 86, 061102, (2005).

[55] C.L. Yang, H.T. He, Lu Ding, L.J. Cui, Y.P. Zeng, J.N. Wang, and W.K. Ge, *Phys. Rev. Lett.*, 96, 186605, (2006).

[56] K.S. Cho, Y.F. Chen, Y.Q. Tang, and B. Shen, *Appl. Phys. Lett.*, 90, 041909, (2007).

[57] L.E. Golub, *Phys. Rev.* B 67, 235320, (2003).

[58] N.S. Averkiev, L.E. Golub, and M. Willander, *J. Phys.: Condens. Matter*, 14, R271, (2002).

[59] N.S. Averkiev, and M.I. D'yakonov, *Fiz. Tekh. Poluprov*., 17, 629, (1983) [Sov. *Phys.Semicond.*, 17, 393, (1983)].

[60] A.A. Bakun, B.P. Zakharchenya, A.A. Rogachev, M.N. Tkachuk, and V.G. Fleisher, Pis'ma ZhETF 40, 464 (1984) [Sov. JETP Lett. 40, 1293 (1984)].

[61] I. Zutic, J. Fabian, and S. Das Sarma, *Appl. Phys. Lett.*, 79, 1558, (2001).

[62] L.E. Golub, *Pis'ma Zh. Eksp. Teor. Fiz.*, 85, 479, (2007) [*JETP Lett.*, 85, 393, (2007)].

[63] L.E. Vorob'ev, E.L. Ivchenko, G.E. Pikus, I.I. Farbstein, V.A. Shalygin, and A.V. Sturbin, *Pisma Zh. Eksp. Teor. Fiz.*, 29, 485, (1979) [*JETP Lett.*, 29, 441, (1979)].

[64] A.G. Aronov and Yu.B. Lyanda-Geller, *Pis'ma Zh. Eksp. Teor. Fiz.*, 50, 398, (1989) [*JETP Lett.*, 50, 431, (1989)].

[65] V.M. Edelstein, *Solid State Commun*., 73, 233, (1990).

[66] F.T. Vasko and N.A. Prima, *Fiz. Tverd. Tela* 21, 1734, (1979) [Sov. *Phys. Solid State*,,21, 994, (1979)].

[67] A.G. Aronov, Yu.B. Lyanda-Geller, and G.E. Pikus, *ZhEksp. Teor. Fiz.*, 100, 973, (1991) [Sov. *Phys. JETP*, 73, 537 (1991)].

[68] A.V. Chaplik, M.V. Entin, L.I. Magarill *Physica E*, 13,744, (2002).

[69] F.T. Vasko and O.E. Raichev, "Quantum kinetic theory and applications", Springer, New York, (2005).

[70] S.A. Tarasenko, *Pis'ma Zh. Eksp. Teor. Fiz*., 84, 233, (2006) [*JETP Lett*., 84, 199, (2006)].

[71] M. Trushin, J. Schliemann, *Phys. Rev. B*, 75, 155323, (2007).

[72] O.E. Raichev, *Phys. Rev. B*, 75, 205340, (2007).

[73] A.Yu. Silov, P.A. Blajnov, J.H. Wolter, R. Hey, K.H. Ploog, and N.S. Averkiev, in *Proc. 13th Int. Symp. Nanostructures: Phys. and Technol*., St. Petersburg, Russia, (2005).

[74] V. Sih, R.C. Myers, Y.K. Kato, W.H. Lau, A.C. Gossard, and D.D. Awschalom, *Nature Physics*, 1, 31, (2005).

[75] N.P. Stern, S. Ghosh, G. Xiang, M. Zhu, N. Samarth, and D.D. Awschalom, *Phys. Rev. Lett.*, 97, 126603, (2006).

[76] S.A. Tarasenko and N.S. Averkiev, *Pis'ma ZhETF*, 75, 669, (2002) [*JETP Lett*., 75, 552, (2002)].

[77] W. Knap, C. Skierbiszewski, A. Zduniak, E. Litwin Staszewska, D. Bertho, F. Kobbi, J.L. Robert, G.E. Pikus, F.G. Pikus, S.V. Iordanskii, V. Mosser, K. Zekentes, and Yu.B. Lyanda-Geller, *Phys. Rev. B*,. 53, 3912, (1996).

[78] N.S. Averkiev and L.E. Golub, *Phys. Rev. B*, 60, 15582, (1999).

[79] J. Schliemann, J.C. Egues, and D. Loss, *Phys. Rev. Lett.*, 90, 146801, (2003).

[80] G. Lommer, F. Malcher, and U. RÄossler, *Phys. Rev. Lett.*, 60, 728, (1988).